NON COHERENT SYNTHETIC APERTURE IMAGING

Pierre Alais, Pierre Cervenka, Pascal Challande, Valérie Lesec

Laboratoire de Mécanique Physique
Université Paris 6, CNRS UPRES A 7068
2 Place de la Gare de Ceinture, F-78210 Saint-Cyr-l'Ecole

INTRODUCTION

A first realization of a synthetic aperture sonar has been related at the third Symposium of Acoustical Holography by Castella [1]. Like in synthetic aperture radar imaging, the acoustical echographic information is added coherently in terms of the complex amplitude obtained from a quadrature synchronous detection at different positions of the emitter/receiver system. The synthetic aperture is limited by the directivity of the emitter and the angular acceptance of the receiver. This technique leads to a transverse or azimutal spatial resolution length Δx which remains independent of the slant range and, in general, much smaller than with a real aperture technique. A classical paper by Cutrona [2] in 1976 discusses the performance of such a technique compared with the classical one. Among the encountered difficulties are : The motion compensation which must be performed within a fraction of a wavelength in terms of the acoustical path ; The spatial sampling which must not create blurring grating lobes and limits severely the speed of exploration. A lot of work has been devoted these last years to this very promising technique [3, 4, 5]. It seems that through new self-focusing algorithms, the perturbations of the vehicle motion can be compensated adequately, but for the yaw which must be known very accurately. Nevertheless, the speed of exploration remains limited and this technique seems adapted to high resolution surveys at the expense of low coverage rates.

Another synthetic aperture technique consists of adding the echographic information received in terms of energy rather than in terms of complex amplitude. The synthetic aperture is limited exactly as in the preceding case, but the phase information is not taken into account : This operation can be defined as a non coherent synthetic aperture imaging technique. In fact, the first author to use this technique was probably Kossoff. In the 1970's [6], he obtained the first good obstetrical ultrasonic images by using, with a manual echographic system, a compound scanning permitting to look at the same target from several angles of view. The compound scanning technique was not used in later systems, including real time electronically scanned systems, because of tissue inhomogeneities which limit the good superposition of images obtained from different azimuths.

Acoustical Imaging, Volume 24.
Edited by Hua Lee, Kluwer Academic/Plenum Publishers, 2000.

The situation is much more favorable in the ocean and the object of this paper is to show that the non coherent synthetic aperture technique, also called "multi-look", if less ambitious than the coherent technique in resolution capability, offers many practical advantages. This technique has been already discussed, at least theoretically, by several authors [7, 8]. H. Lee [9] gives experimental results that compare the multi-look sonar technique with the classical one and also with the coherent synthetic aperture technique. It is well recognized that the non coherent addition of echographic information does not permit to improve substantially the resolution. The focusing effect created in such a way is related to the temporal resolution or to the corresponding range resolution length Δy. A crude model, based on a rectangular profile for an echographic information obtained without any other focusing technique, yields a focusing effect characterized by the following approximate resolution length :

$$\Delta x_{3dB} = 4\Delta y/\Delta\theta\,, \tag{1}$$

where $\Delta\theta$ is the acceptance angle permitted by the echographic system for operating the synthetic addition (Figure 1).

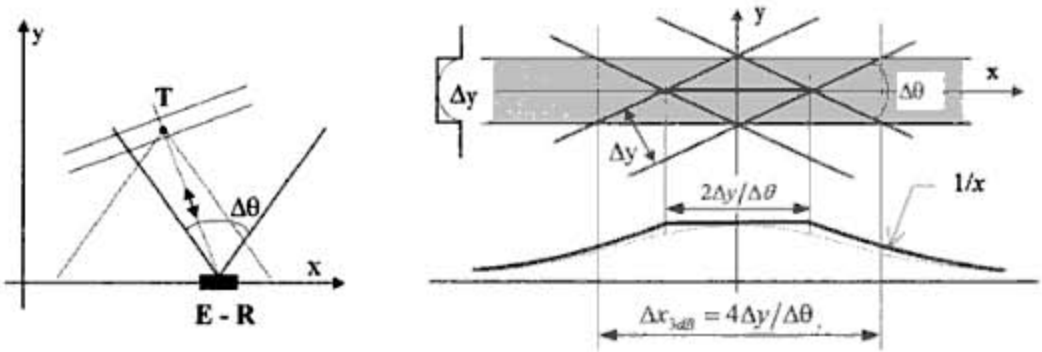

Figure 1 : Focusing by a non coherent synthetic aperture addition of energy

If the operation is performed with a receiving array of real aperture $L = pa$ (p adjacent elements of size a), the focusing capability of the physical antenna (coherent real aperture) at a slant range R is expressed by $\Delta x_{3dB} = R\lambda/L$. The receiving angle of view is classically limited by $\Delta\theta_{max} = \lambda/(2a)$ to keep grating lobes at a reasonably low level. Let us denote $N = L/\lambda$ and $n = a/\lambda$, respectively the length of the array and the width of the each array element measured in wavelengths λ. The focusing effects by non coherent synthetic aperture and by coherent real aperture become equal for the slant range R given by :

$$R = 8\,Nn\,\Delta y \tag{2}$$

It is easy to check that for practical cases, the non coherent synthetic aperture effect is not efficient in terms of resolution as it will be seen in one particular experiment. Hence, it remains important to use a high resolution real aperture system : The synthetic operation affords a small improving effect on the resolution Δx, and at large ranges only.

In fact, our paper aims to show that the non coherent synthetic addition has many other advantages than increasing the focusing effect. The greatest improvement occurs in the image quality because of the contrast enhancement : The non coherent summation cancels the speckle effect induced by the coherent process performed on the physical antenna. Another great advantage is the robustness of this technique with respect to motion perturbations. Errors in the estimation of the motion may be accepted with one or two orders of magnitude larger than in the coherent synthetic aperture process. Spatial under-sampling of pings caused by the vehicle speed is also well tolerated and allows large coverage rates.

THE EXPERIMENTAL SYSTEM

We have built a single sided prototype sonar. The transmitted signal is a linear FM chirp (F_o = 100 kHz, B = 3 kHz) whose amplitude is modulated with a truncated Gaussian window. The range resolution obtained after pulse compression is about 30 cm. The aperture in site is classical for both transmitter and receivers, but the transmitted beam is rather large in azimuth ≅ 10°, obtained by means of a transmitting antenna whose geometry is an arc of circle (radius ≅ 6 m, curvilinear length ≅ 1.3 m). Two linear arrays are used at receive for interferometric purpose and bathymetric measurements. Each array (L = 1.44 m ≅ 96 λ) is composed of 32 transducers (a = 45 mm ≅ 3 λ). The resulting angular resolution is about 0.7°. In these conditions, the maximum angle of view maintaining the grating lobes at reasonable levels is $\Delta\theta = \lambda/(2a)$ = 1/6 rad., i.e. the 10° adopted for the transmitted beam.

According to Eq. (2), the range for which the synthetic addition may be effective is 800 m, so that we can expect only a small improvement for the spatial along track resolution Δx. The following simulation will confirm this situation, but will show also how the speckle is washed out in comparison with conventional imaging technique.

SIMULATIONS

A single point target is assumed to be located at 600 m range. Figure 2 is the image of this target obtained with a single ping. The receiving array is not tapered, so that the first side lobe level is at –13 dB. Figure 3 is the image of the same target obtained after non coherent processing of simulated pings covering a tapered angular aperture of 10° @ –6 dB (length of the simulated trajectory = 105 m). The combination of the high range resolution (thanks to the pulse compression technique) with the rotation that the multi-look angles, results in the scattering of the side lobes whose levels are therefore reduced (–5 dB for the first lobe, –7 dB for the second lobe). A slight gain for the angular resolution (14% @ –6 dB) can be also observed. The larger the target range and the synthetic angular aperture, the most effective is the process with respect to the reduction of the side lobes level and the increase of the resolution.

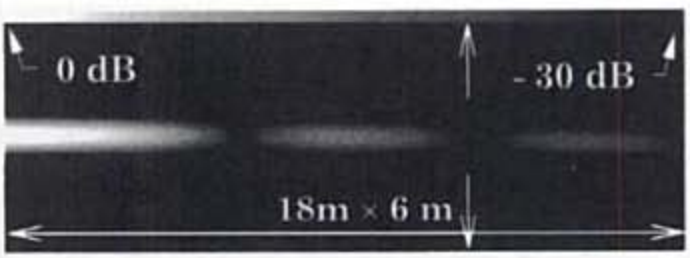

Figure 2 : (half) Point Spread Function - Single ping (target @ 600 m)

Figure 3 : Non coherent synthesis (10° aperture @ –6 dB ≡ 105 m baseline)

A simple configuration is used in Figures 4-6 to show the mechanism of the speckle reduction. We assume two closely spaced point targets (40 cm apart) at 200 m range. In Figure 4, the targets are perfectly symmetrical to the bore-sight direction of the single ping used to build the image. The targets cannot be discriminated by the receiving antenna. They produce a single central spot together with side lobes. In Figure 5, the targets are slightly rotated, so that the range difference is $\lambda/4$, i.e. only 3.25 mm ! Now, the antenna lies in between two petals of the backscattered diagram. Because the size of the antenna is large enough to cover a significant part of a petal, the image is not completely black. The central spot is divided in two parts, resulting of an interference process. These two spots are not actual images of the targets which are much closer. Figure 6 shows the image obtained after a non coherent summation of pings such as for building Figure 3. Both unresolved targets are seen as a single spot. A single image is displayed here, because there is absolutely no difference whether the targets are perfectly symmetrical or not. The cause is that the base-line of the non coherent process encompasses in both cases several petals of the diagram. The only noticeable effect is a constant loss of about 5 dB which corresponds roughly to the normalized mean energy returning from a petal.

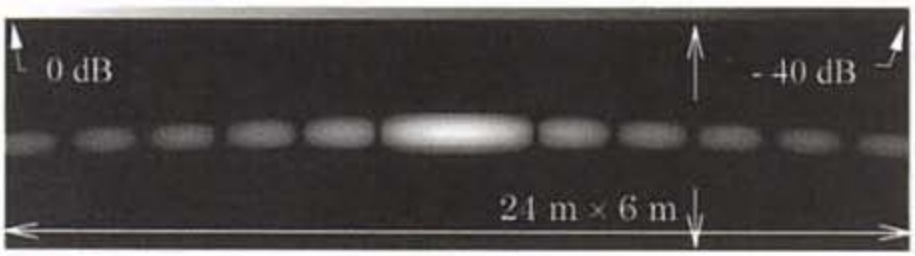

Figure 4 : Central ping - Symmetrical targets (40 cm apart) @ 200 m range

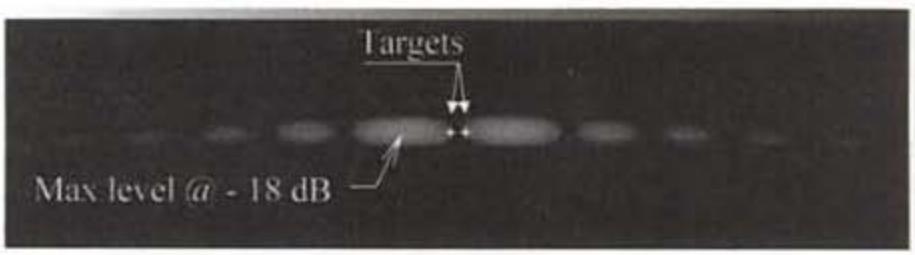

Figure 5 : Central ping - Targets range difference = $\lambda/4$

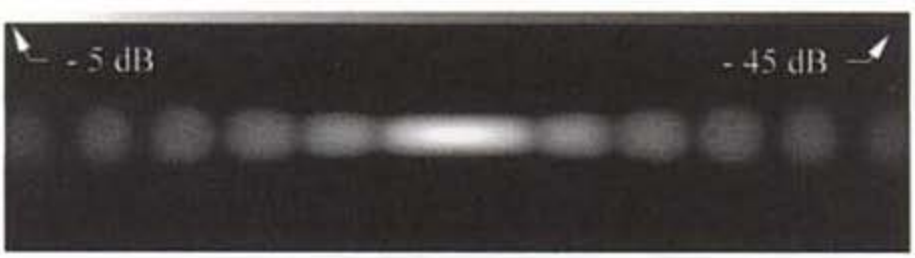

Figure 6 : Non coherent synthesis (10° aperture) - Distance between targets = 40 cm

EXPERIMENTAL RESULTS

Our experimental results have been obtained at the GESMA (Groupe d'Etudes Sous-Marines de l'Atlantique) facility in the bay of Brest. It consists of an horizontal rail that carries a motorized sliding platform. The translation capability is 12 m. The rail is mounted on a dock open to the sea, and may be immersed at different depths. The antenna was about 3 m below the sea surface and 9 m above the bottom. The bore-sight direction aimed at 40° below the horizontal. In this area, the sea bottom is nearly flat. Several objects were set on the bottom, and particularly a cylinder (70 cm diameter, 1,9 m long) at 30 m range and a sphere (1 m diameter) at 50 m range. This range is very small compared to what can be expected at a frequency of 100 kHz, but is convenient with respect to the practical limitation (< 12 m) of the synthetic aperture and the value retained for the angle of view (10°).

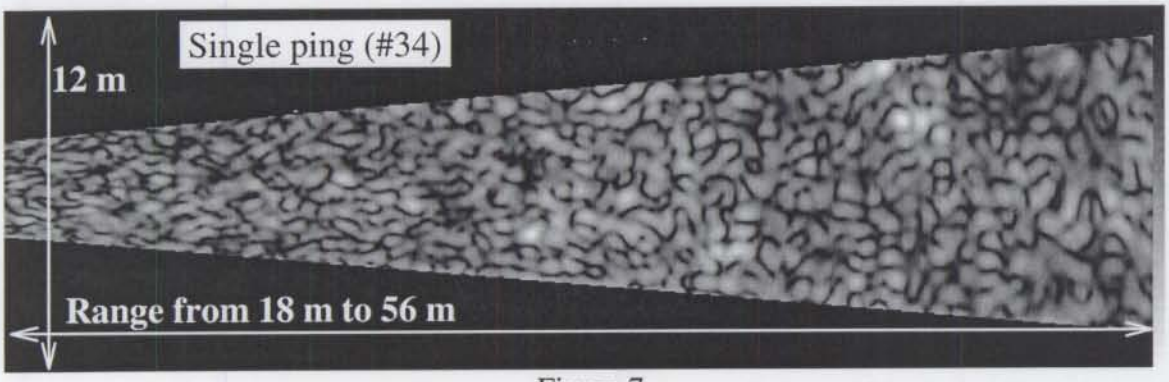

Figure 7

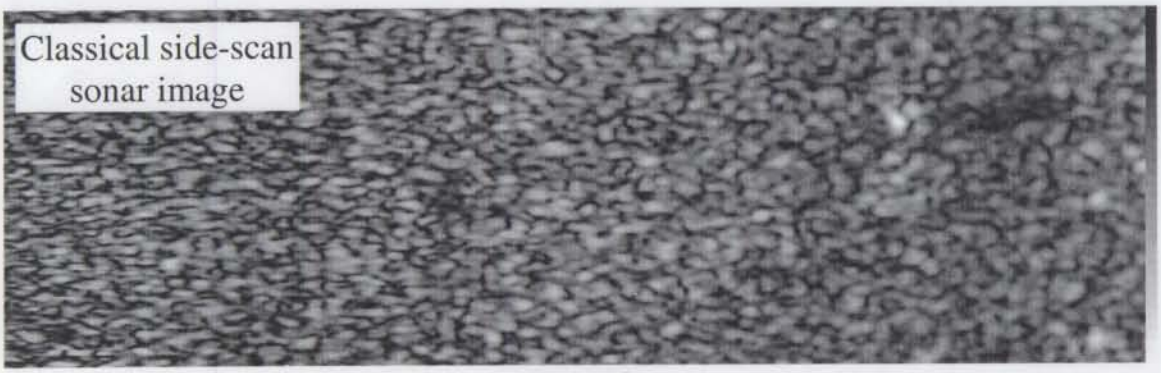

Figure 8

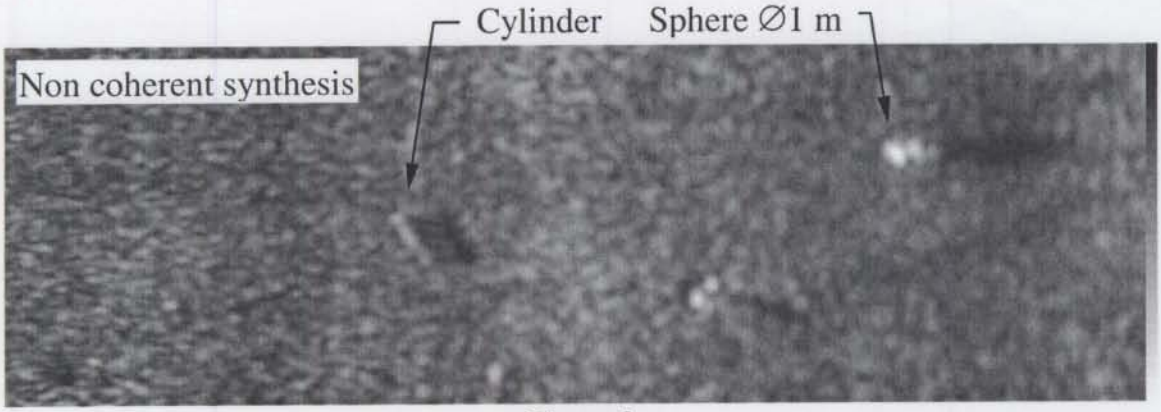

Figure 9

With a first mode of data acquisition, base-band digitized signals received by each of the 32 transducers of a single array were registered. The presented images are computed with these data sets. The representation is in slant range, i.e. there is no radiometric correction. The pixel dimension is 5×5 cm^2. For comparison purpose, the median gray level is adjusted at 35%. No histogram equalization, nor other fancy image enhancement, are performed.

Figure 7 exhibits the image computed with a single ping (shot from the center of the rail). The speckle noise hides most of the features : The echoes from the sphere can be only guessed. Figure 8 is built as a classical side-scan sonar image, i.e. signals received from each ping at bore-sight are properly merged and smoothed. The shadow of the sphere can be seen, and the presence of the cylinder can be guessed. However, the presence of the speckle noise is still very perturbing. Figure 9 is obtained after non coherent processing of all pings, i.e. adding the energy of images such as shown in Figure 7, using a tapered aperture of 10° width @ -6 dB. The size of the sphere is close to the limit of resolution of the receiving antenna. However, the drastic reduction of the speckle noise exemplifies the clear advantage afforded by this technique. The shadows of the cylinder and of the sphere appear clearly.

Let us define the redundancy factor, r, as the number of pings that can be used to build a pixel at a given range $R \leq R_{max}$, i.e. :

$$r = (R/R_{max})\,(c\Delta\theta/2V) \qquad (3)$$

where R_{max} is the maximal slant range, V is the speed of the platform and $\Delta\theta$ is the synthetic angular aperture.

In Figure 9, the conditions are ideal because 60 shots were used on the imposed linear trajectory of 12 m run at low speed (20 cm/s). However, it must be noted that the redundancy factor can be drastically reduced, down to 5. We checked that Figure 9 is only slightly degraded if we use only 6 pings instead of 60. Only zones at very close range are possibly under-sampled. For example, the condition $r > 5$ is satisfied for a vehicle that runs at 6 knots, 100 m above the sea bottom, looking up to $R_{max} = 1000$ m, with a view angle $\Delta\theta = 5°$. In these conditions, the Doppler shift would remain less than 12 Hz, and would afford an equivalent perturbation of 40 mm in the acoustical path with the used chirp. This perturbation is much smaller than the range resolution, so that the Doppler effect would not affect the image quality.

Besides, as mentioned in the introduction, the non coherent technique is very robust with respect to the perturbations induced by the vehicle motion. Figure 10 is built with a bias in the lateral speed of the antenna, i.e. by taking a value that is not null. Such a bias is almost equivalent to introducing a bias in the azimuth. A very large value (16 cm/s @ 2 knots ≡ 9°) has been chosen in order to see some significant difference with the reference image (Figure 11). Another major source of artifact occurs from the bias in the measurement of the rotation speed. Here again, a large value has been chosen to build Figure 12 (1.2° between extreme pings, 0.1°/s @ 2 knots) in order to induce a significant blurring effect. It must be noticed that the image obtained by coherent synthesis (Figure 13 - coherent synthetic aperture over 4° @ -6 dB) is completely destroyed if such biases are introduced.

On the other hand, our system is able to record on line the information corresponding to 15 directions in azimuth, with an angular pitch of .66° in order to cover the entire view angle $\Delta\theta$. These preformed beams use 8 focal zones to keep the best azimuth resolution in the range 10 m – 1000 m. This information permits to build images with a very low degradation compared to Figure 9, with much less computation and much higher speed.

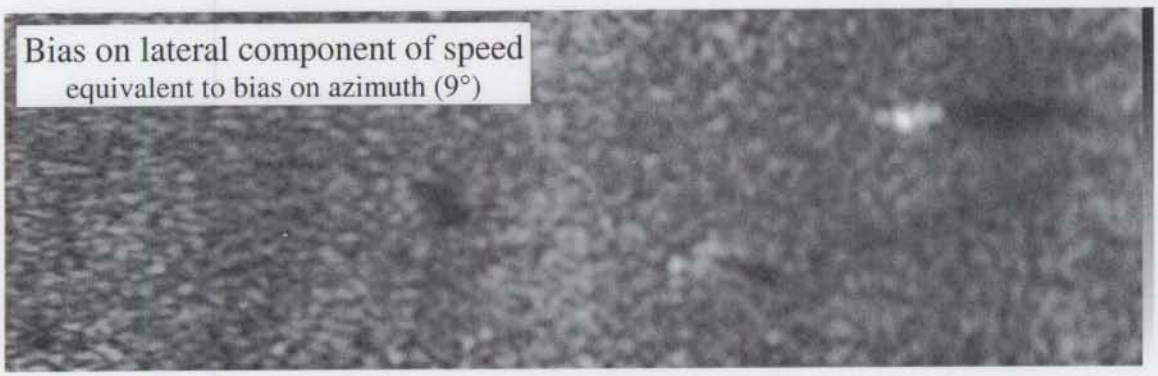

Figure 10

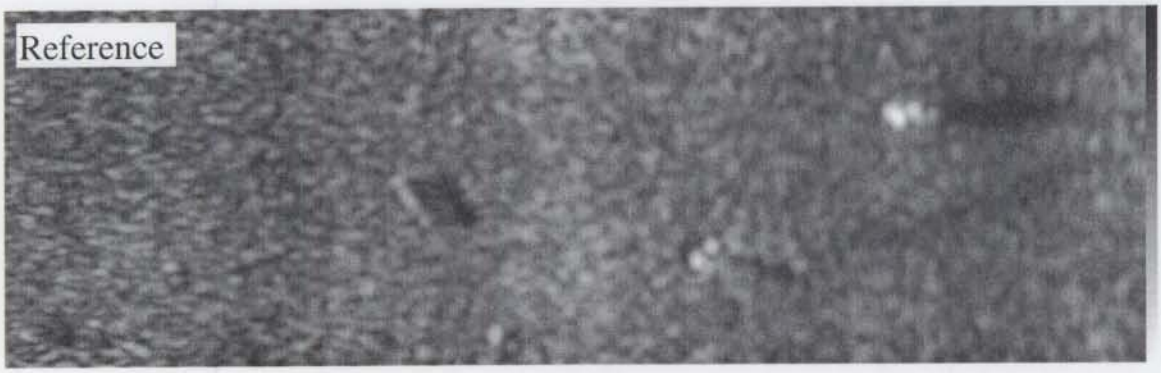

Figure 11

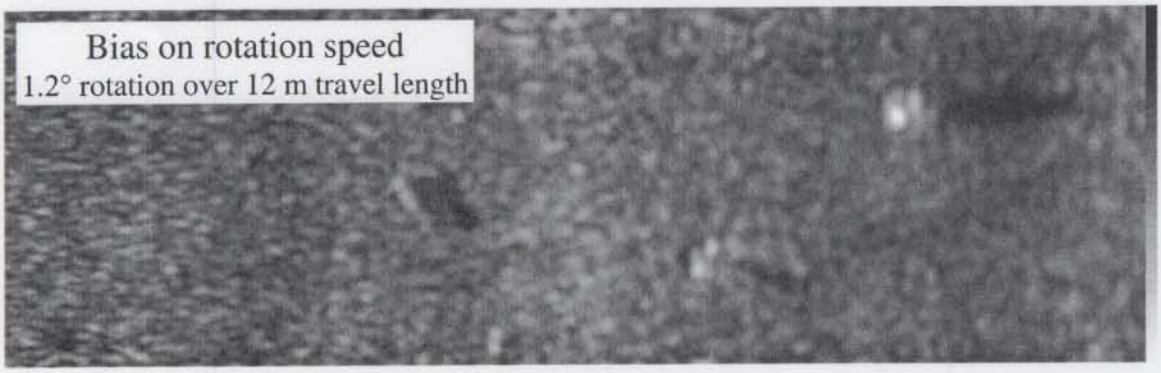

Figure 12

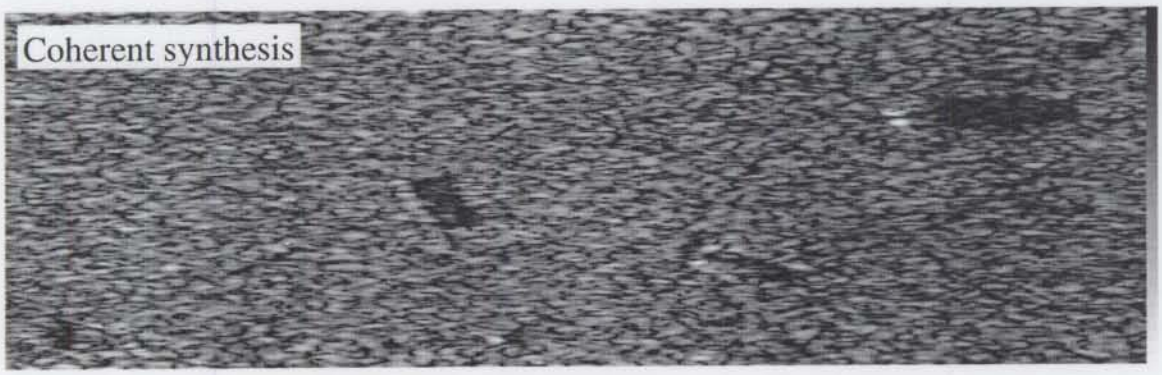

Figure 13

CONCLUSION

The non coherent imaging technique does not aim at the same goal as the coherent synthesis. With the non coherent process, the overall resolution is not much increased with respect to the theoretical performance of the physical array. However, the image quality is definitively improved at a low computational expense, and without stringent requirements about the accuracy of the antennae trajectory and attitude.

The main interests for the non coherent synthesis are : 1) Reduction of the side lobe levels, together with a slight improvement of the resolution in azimuth ; 2) Drastic reduction of the speckle effect so that objects whose size is close to the theoretical longitudinal resolution of the physical antennae can be detected ; 3) Robustness of the image quality with respect to the trajectory and attitude artefacts ; 4) Robustness of the image quality with respect to the vehicle speed as long as the redundancy factor remains larger than 5, which authorizes surveys at high coverage rate ; 5) Improvement of bathymetric measurements through the redundancy factor. This effect will be shown in an other paper. We are looking now for an experiment carried from a vessel, in order to verify and to quantify the capabilities of this technique at larger ranges, i.e. in actual operational conditions.

ACKNOWLEDGMENTS

We thank M. Brussieux, V. Tonard and A. Salaun from GESMA for their very efficient cooperation for carrying the experiments in Brest.

REFERENCES

1. F.R. Castella, *Application of one-dimensional holographic techniques to a mapping sonar system*, Acoustical Holography, Vol. 3, 1970, pp. 247-271.
2. L.J. Cutrona, *Comparison of sonar system performance achievable using synthetic aperture techniques with the performance achievable by more conventional means*, J.A.S.A., Vol. 58, n° 2, August 1975, pp. 336-348.
3. J. Chatillon, M.E. Zakharia, M.E. Bouhier, *Self-focusing of synthetic aperture sonar : validation from sea data*, Proc. 2nd European Conference on Underwater Acoustics, Lyngby, Denmark, July 1994, pp. 727-731.
4. V. Tonard, J. Chatillon, *Acoustical imaging of extended targets by means of synthetic aperture sonar technique*, Acustica, Acta Acoustica, Vol. 83, 1997, pp. 992-999.
5. D. Billon, F. Fohanno, *Theoretical performance and experimental results for synthetic aperture sonar self-calibration*, Oceans'98, Septembre 1998, Nice, France.
6. G. Kossoff, *Progress in pulse echo techniques*, Proc. 2nd World Congress Ultrasonics in Medicine, Rotterdam 1974, pp. 37-48.
7. M.P. Hayes, P.T. Gough, *Broad band synthetic aperture sonar*, IEEE Journal of Oceanic Engineering, Vol. 17, n° 1, Janvier 1992.
8. G. Shippey, T. Nordkvist, *Phased array acoustic imaging in ground coordinates, with extension to synthetic aperture processing*, IEEE Proc. Radar Sonar Navigation, Vol. 143, n° 3, Juin 1996.
9. B.L. Douglas, H. Lee, C.D. Loggins, *A multiple receiver synthetic aperture active sonar imaging system*, Oceans'92, Conf. Records MTS, IEEE, 1992, pp. 300-305.